

## A comparative study of Schiff base chelating resins: synthesis, uptake of heavy metal ions, and thermal studies

Fatma A. Al-Yusufy<sup>1</sup>, Mohammed Q. Al-Qadasy<sup>1</sup>, Yasmin M. S. Jamil<sup>1</sup>, Hussein M. Al-Maydama<sup>1</sup>, Moathe M. Akeel<sup>1</sup>

<sup>1</sup>Sana'a University, Faculty of Science, Department of Chemistry, Sana'a, Yemen

\* Corresponding author: Fatma A. Al-Yusufy, e-mail address: [f\\_aljusufy@yahoo.com](mailto:f_aljusufy@yahoo.com)

### ARTICLE INFO

#### Article history:

Received: February 5, 2018

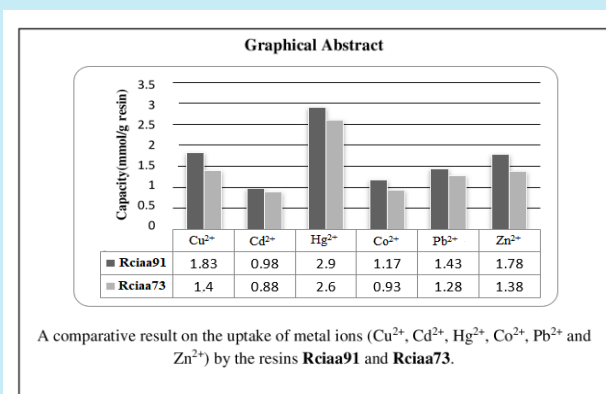
Accepted: May 7, 2018

Published: August 23, 2018

#### Keywords:

1. Schiff bases
2. chelating resins
3. cross-linking
4. metal ion uptake
5. physical parameters

**ABSTRACT:** Two new chelating resins (**Rciaa91** and **Rciaa73**) with different compositional chelating groups and degree of cross-linking were prepared by free radical copolymerization of Schiff bases obtained from condensation reaction of cinnamaldehyde (ci) with anthranilic acid (aa) and 1,4-phenylenediamine (pn) monomers. The synthesized materials were characterized using CHN analyses, FTIR, <sup>1</sup>H-NMR, and thermal analyses (TGA, DTA). Batch technique was applied, and the contact time, pH and initial concentration of the metal ions were investigated as factors affecting the uptake behavior. The results obtained indicated that the chelating resin with larger compositional ratio of chelating moieties and lower degree of cross-linking showed lower optimum reaction time and higher uptake affinity towards the metal ions Cu(II), Cd(II), Co(II), Zn(II), Hg(II), and Pb(II), under the same conditions. Both the chelating resins showed uptake behavior of the metal ions in the following order  $Hg^{2+} > Cu^{2+} > Zn^{2+} > Pb^{2+} > Co^{2+} > Cd^{2+}$  each metal at its optimum pH and at the same reaction time and ion concentration. The thermal degradation behavior and stability of the resins were investigated by using non-isothermal thermogravimetric analysis (TGA/DTG/DTA), at 10 °C min<sup>-1</sup> heating rate and under nitrogen. The Coats-Redfern method was used to evaluate the kinetic and thermodynamic parameters ( $\Delta G^*$ ,  $\Delta H^*$  and  $\Delta S^*$ ) for the prominent degradation steps in the TGA curves at 450-660 °C range.



### 1. Introduction

The removal and separation of metal ions in aqueous solution play an important role for the analysis of wastewaters, industrial and geological samples as well as for environmental remediation<sup>1, 2</sup>. Chelating resins have been widely utilized for the removal of the undesired metal ions from these aqueous solutions<sup>3, 4</sup>. The development of high performance chelating resins for removing heavy metal ions from aqueous solution is considered not only as research priority in the environmental field but also as an area of interest in inorganic catalyst and recovery of valuable trace

metal ions<sup>5-8</sup>. These resins show greater selectivity compared to the conventional types of ion exchangers<sup>9-11</sup>. Besides, they show good physical and chemical properties such as porosity, high surface area, durability and purity<sup>12-14</sup>. Many chelating resins with different functionalities like quaternary amine<sup>11, 12</sup>, sulfonamides<sup>15</sup>, Schiff base<sup>7, 8, 16-20</sup>, sulfonic acid<sup>21</sup>, hydroxamic acid<sup>22</sup> and amidoxime<sup>23, 24</sup> have been emphasized for interaction with metal ions.

Schiff bases having multidentate coordination sites are known to form complexes with transition metal ions readily. Present in a polymer matrix, they are expected to show affinity and selectivity

towards the metal ions at an appropriate pH<sup>7,8,16-20</sup>. This led us to synthesize chelating resins, which will show affinity for the metal ions at appropriate pH.

In the present work Schiff base chelating resins have been prepared. The adsorption behavior of the resin obtained towards heavy metal ions (II); Cu, Cd, Co, Zn, Hg, and Pb have been studied. Both kinetic thermodynamic parameters of the adsorption process were also calculated. It also reported the thermal behavior, degradation kinetic, thermodynamic parameters and the thermal stability of the **Ricaa91** and **Ricaa73** resin at a single heating rate (10 °C min<sup>-1</sup>).

## 2. Experimental

### 2.1 Chemicals

All starting materials were reagent grade: solvents, indicators and metal ions (Cu<sup>2+</sup>, Cd<sup>2+</sup>, Co<sup>2+</sup>, Zn<sup>2+</sup>, Hg<sup>2+</sup>, and Pb<sup>2+</sup>) were purchased from BDH chemical company - England, anthranilic acid, and absolute ethanol from Fluka chemical company-USA, 1,4-phenylenediamine and benzoyl peroxide from Aldrich chemical company-Germany, and cinnamaldehyde and 1,2 azobisisobutyronitrile (AIBN) were from HiMedia laboratories- India.

Anthranilic acid was purified and recrystallized before use from distilled water. 1,4-Phenylenediamine was recrystallized from benzene. Cinnamaldehyde and 1,2 azobisisobutyronitrile were used as received.

### 2.2 Techniques

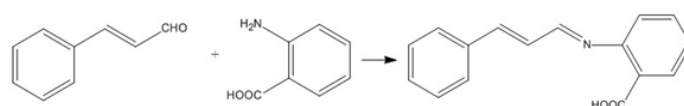
Melting points were determined on Stuart Scientific Electro-thermal melting point apparatus. FTIR spectra were recorded using the KBr disc technique on a JASCO 410 FTIR Spectrophotometer. Elemental analyses (CHN) were performed on an elemental analyses system, GmbH VARIOEL V<sub>2,3</sub>1998 CHNS Mode. <sup>1</sup>H-NMR spectra were recorded in d<sub>6</sub> DMSO on VARIAN 300 MHz FT-NMR Spectrometer (δ in ppm) using TMS as an internal reference. The TGA/DrTGA, DTA/DrDTA thermo-analytical curves were measured in a heating range (25-800 °C) and at a rate of 10 °C min<sup>-1</sup> under nitrogen using Shimadzu TGA-50H and Shimadzu DTA-50H thermal analyzers, respectively.

### 2.3 Synthesis of Schiff bases

#### 2.3.1 Synthesis of cinnamaldehyde anthranilic acid (*ciaa*)

The Schiff base **ciaa** was prepared by adding cinnamaldehyde (0.05 mol, 6.38 mL) to solution of anthranilic acid (0.05 mol, 6.86 gm) in 20 mL absolute ethanol with stirring and gentle heating. The formed precipitate was filtered, washed with ethanol and then dried in air (Scheme 1). Color yellow. Mwt. 251. Yield 85%. M.p. 140 °C.

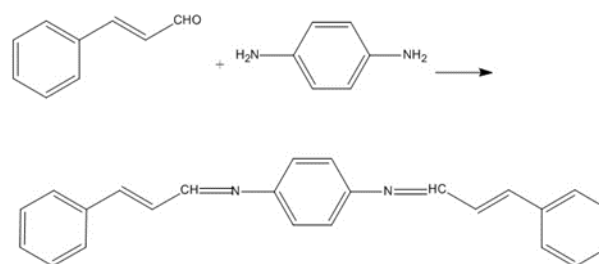
Elemental analysis (% CHN): Calcd. (Found) C: 76.47 (76.23), H: 5.21 (5.07), N: 5.57 (5.32). <sup>1</sup>HNMR data (DMSO-d<sub>6</sub>): (ppm), 4.7 - 8.00 (m, CH vinyl, CH arm), 9.65(d, CH=N). IR (KBr) v/cm<sup>-1</sup>: 3100 - 2634 (broad band OH<sub>str</sub>), 3063, 3029 (=CH vinyl, arm), 1704 (C=O), 1616 (CH=N), 1603, 1586, 1509 (C=C vinyl, arm), 747, 687 (=CHoop).



Scheme 1: Synthesis of the Schiff base **ciaa**

#### 2.3.2 Synthesis of cinnamaldehyde-1,4-phenylenediamine (*cipn*)

To a solution of 1,4-phenylenediamine (0.05 mol, 5.41gm) in 20 mL absolute ethanol, a cinnamaldehyde (0.1 mol, 12.7 mL) was added with stirring and gentle heating. The precipitate obtained was filtered, washed thoroughly with ethanol and then dried in air (Scheme 2). Color, pale yellow. Mwt. 336. Yield 80%. M.p. 227 °C.



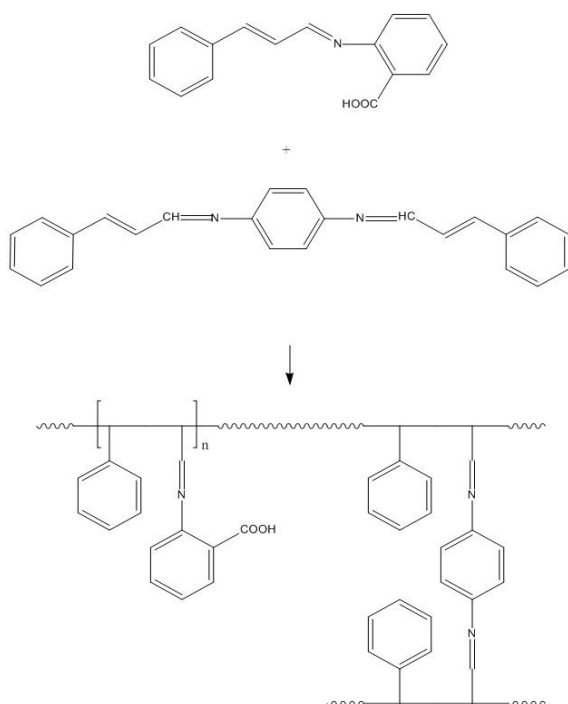
Scheme 2: synthesis of the Schiff base **cipn**.

Elemental analysis (% CHN): Calcd. (Found) C: 85.68 (85.06), H: 5.99 (5.86), N: 8.32 (7.90). <sup>1</sup>HNMR data (DMSO-d<sub>6</sub>): δ(ppm), 7.1 - 7.6 (m, CH vinyl, CH arm), 8.4 (d, CH=N). IR (KBr) v/cm<sup>-1</sup>

<sup>1</sup>: 3077, 3039, 3029 (=CHstr), 1626 (CH=N), 1603, 1599, 1586, 1572 (C=C vinyl, arm), 838, 745, 693(=CHoop).

#### 2.4 Synthesis of (*ciaa* – *cipn*) copolymers (chelating resins)

A general heterogeneous copolymerization method was used in the preparation of the chelating resins in this study<sup>25</sup>. Each of the comonomers, **ciaa** and **cipn**, were mixed individually with AIBN (1 mol/100 mol of common mixture) as a polymerization initiator in 5 mL DMF. The radical copolymerization was maintained by mixing together the two comonomer mixture solutions, then heating to 75 °C under reflux for 24 h. After cooling the chelating resin was precipitated in methanol, filtered off, washed several times with methanol and finally, dried in air (Scheme 3). Since the Schiff base **cipn** possess two vinyl (-CH<sub>2</sub>=CH<sub>2</sub>-) moieties on either sides of its chemical structure, it was deliberately used as the cross-linking agent in the preparation of the chelating resins.



**Scheme 3:** Synthesis of Schiff base chelating resins, **Rciaa91** and **Rciaa73**.

The resin of (*ciaa-cipn*) copolymer was prepared as crosslinked chelating resins in two different ratios of **ciaa** and **cipn** mixtures<sup>26</sup>; a mixture of **ciaa** (9 gm, 35.9×10<sup>-3</sup> mol) and **cipn** (1

gm, 3×10<sup>-3</sup> mol) to form the resin **Rciaa91**, and that of **ciaa** (7 gm, 27.9×10<sup>-3</sup> mol) and **cipn** (3 gm, 8.9×10<sup>-3</sup> mol) to form the resin **Rciaa73**.

#### 2.5 Metal ion adsorption measurements using a batch method.

Stock solutions of the metal ions were prepared in distilled water. A stock solution of EDTA (5.0 × 10<sup>-3</sup> mol L<sup>-1</sup>) was prepared and standardized against a solution of MgSO<sub>4</sub>·7H<sub>2</sub>O using Eriochrome Black-T (EBT) as an indicator<sup>27</sup>. Buffers of acetic acid/sodium acetate and ammonium hydroxide/ammonium chloride were used for the experiments carried out under a controlled pH.

The metal ion adsorption experiments using the batch method were carried out at a controlled pH by placing 0.05 g chelating resin with 50 mL metal ion at initial concentration 5.0 × 10<sup>-3</sup> mol L<sup>-1</sup>. The contents of the flask were equilibrated on a Gallenkamp flask shaker at room temperature for 60 min at 150 rpm. The pH of the solution was adjusted using a suitable buffer. Then, 5 mL of the solution (free of suspended solid) were taken at the end of the experiment at different intervals. The residual concentration of the metal ion solution was determined via titration against 5.0 × 10<sup>-3</sup> mol L<sup>-1</sup> EDTA using EBT indicator<sup>27,28</sup>.

#### 2.6 Effect of pH on the uptake of metal ions

The effect of pH of the metal ion test solution is an important parameter for adsorption of metal ions because it affects the solubility of the metal ions, concentration of the counter ions, on the functional groups of the adsorbent and the degree of ionization of the adsorbent<sup>29</sup>. Adsorption measurements under pH control were carried out following the above procedures of uptake experiments. The pH was controlled using NH<sub>4</sub>OH/NH<sub>4</sub>Cl buffer solution to study the uptake behavior at the alkaline mediums (pH 6–12) and acetic acid/sodium acetate (AcOH/NaOAc) buffer was used to study the uptake in the acidic medium (pH 4).

### 3. Results and discussion

#### 3.1 Synthesis and Characterization

The Schiff bases, **ciaa** and **cipn** were prepared as described in the experimental part, by the reaction of cinnamaldehyde (ci) with anthranilic acid (aa), and 1,4-phenylenediamine (pn), respectively. The Schemes 1 and 2 display the structures of the synthesized Schiff bases **ciaa**, **cipn**, respectively. Two chelating resins, **Rciaa91** and **Rciaa73** were then synthesized using free radical polymerization reaction of the synthesized Schiff bases with different compositional weight ratios (**ciaa:cipn**), 9:1 and 7:3, respectively, (Scheme 3).

The synthesized Schiff bases were subjected to elemental analysis (CHN) and their found values were in good agreement with those of the calculated values for the suggested formulas of the prepared samples. The melting points were sharp, indicating the purity of prepared Schiff bases.

### 3.2 Spectral analysis FTIR spectra

The chemical structures of the synthesized Schiff bases were confirmed by the IR and <sup>1</sup>HNMR spectra. The FTIR spectra of the synthesized Schiff bases, **ciaa** and **cipn**, showed sharp and strong characteristic absorption peaks. Figure 1 displays the FTIR spectra of the synthesized Schiff bases, and their corresponding copolymer **Rciaa91**. The disappearance of the aldehydic carbonyl  $\nu(\text{C}=\text{O})$  band and the amino  $\nu(\text{NH}_2)$  bands of the starting materials, and the appearance of the azomethine  $\nu(\text{C}=\text{N})$  band confirmed the formation of the Schiff bases. The  $\nu(\text{C}=\text{N})$  stretching frequencies of the Schiff bases, **ciaa** and **cipn** appeared at 1616, 1626, respectively. Upon copolymerization of the Schiff bases **ciaa** and **cipn**, the IR spectra of the chelating resins showed broader and less intense peaks compared to their corresponding comonomers. The medium broad peak in the range of 3400 – 3200  $\text{cm}^{-1}$  could be due to the adsorbed water molecules on the Schiff base chelating resin because of its hygroscopic nature<sup>18</sup>.

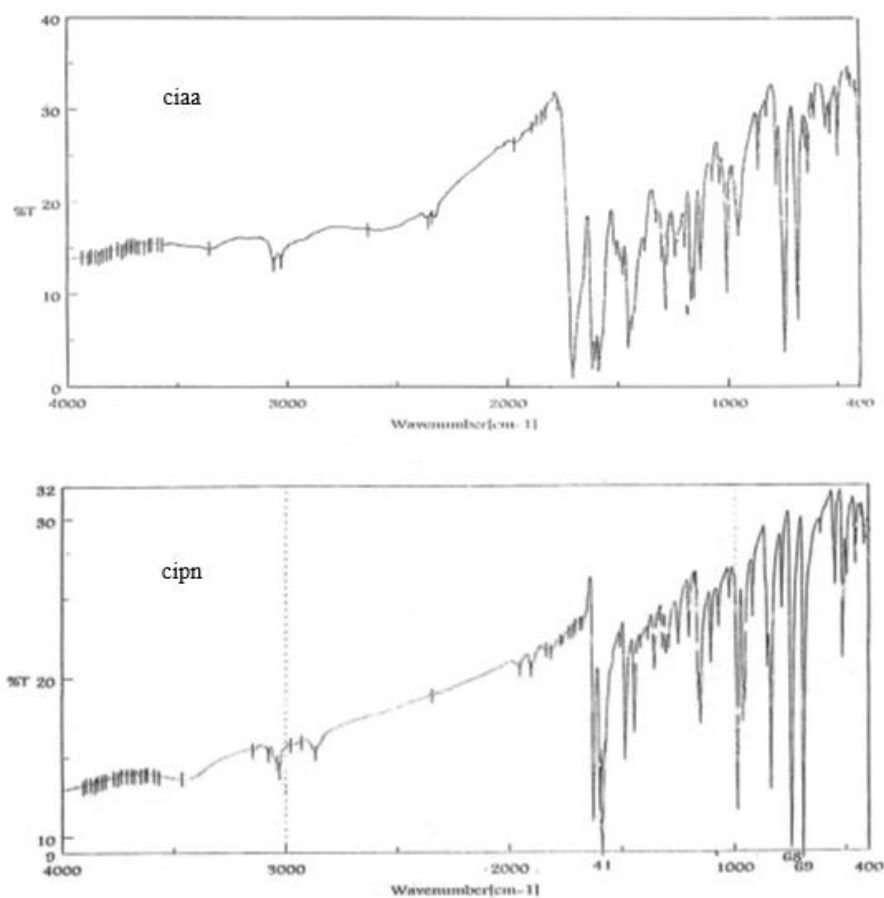


**Figure 1:** FTIR spectra of the Schiff bases, **ciaa** and **cipn**, and the chelating resin **Rciaa91**.

Figure 2 shows the  $^1\text{H}$ NMR spectra of the Schiff base, **ciaa** and **cipn**. The  $^1\text{H}$ NMR spectra of the Schiff bases, **ciaa** and **cipn** showed doublet signals for the  $\delta$  (CH=N) protons at 9.65 and 8.45, respectively. The multiple peaks in the range  $\delta$  6.47 - 8.00 ppm were attributed to the vinyl and aromatic protons of the conjugated structure of the

Schiff bases. The singlet peak at 2.51 ppm in the spectra of is due to the DMSO solvent used in the analysis. The appearance of a broad signal at  $\delta$  3.2 ppm in  $^1\text{H}$ NMR spectrum of the Schiff base **cipn** could be attributed of the presence of traces of unreacted  $\text{NH}_2$  in its chemical structure<sup>30</sup>.

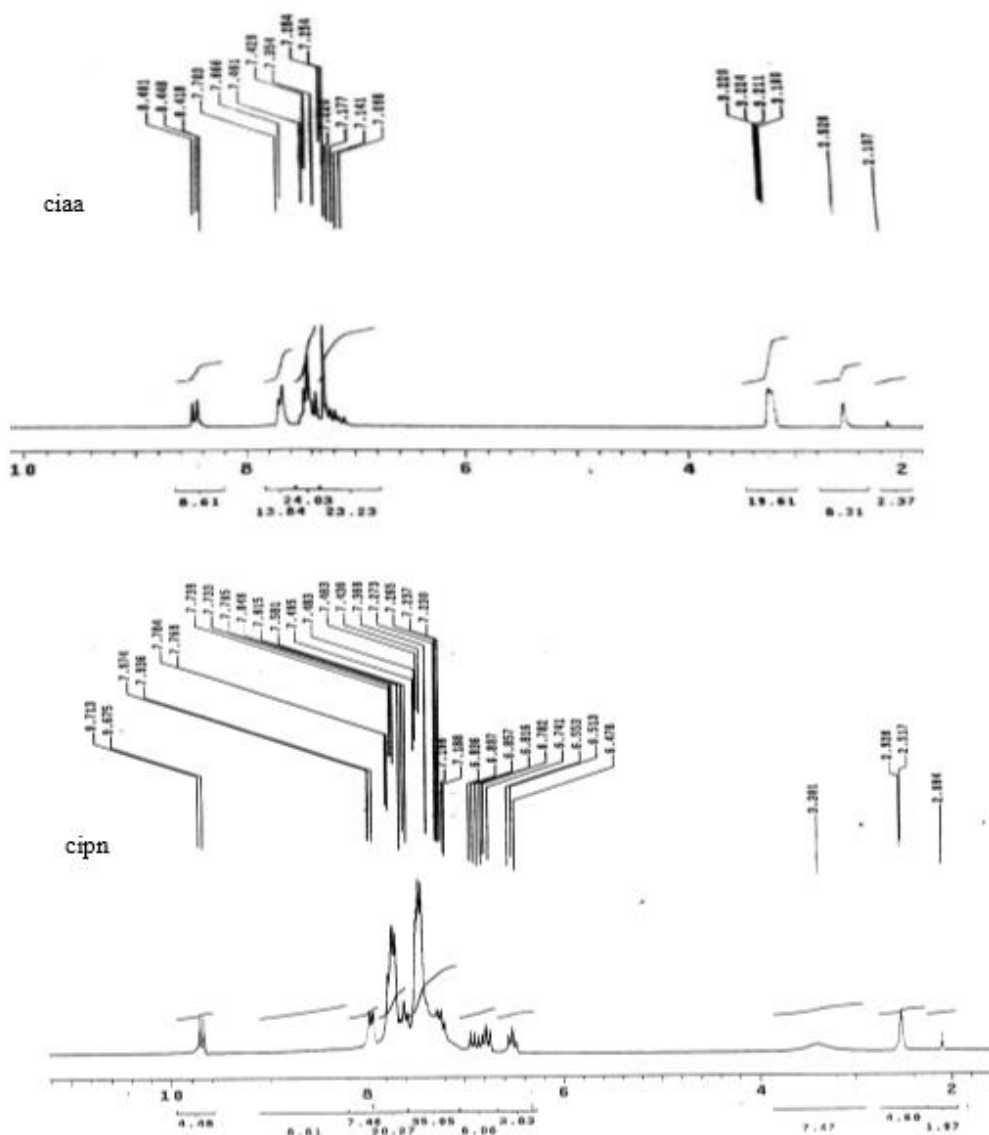


Figure 2:  $^1\text{H}$ NMR spectra of the Schiff bases, **ciaa** and **cipn**.

### 3.3 Uptake of metal ions ( $\text{Cu}^{2+}$ , $\text{Cd}^{2+}$ , $\text{Co}^{2+}$ , $\text{Zn}^{2+}$ , $\text{Hg}^{2+}$ , $\text{Pb}^{2+}$ ) by the chelating resins

#### 3.3.1 Optimum pH of the metal ion uptake

The preliminary uptake experiments of the metal ions;  $\text{Cu}^{2+}$ ,  $\text{Cd}^{2+}$ ,  $\text{Co}^{2+}$ ,  $\text{Zn}^{2+}$ ,  $\text{Hg}^{2+}$  and  $\text{Pb}^{2+}$  by the chelating resin **Rciaa91** and **Rciaa73** at

different pH values between 4 and 10 were examined by batch technique for 60 minutes as a reaction time<sup>26</sup>. The results are shown in Table 1. In general, the uptake of the metal ions increased with increasing pH, until reaching a maximum value and then followed by a decrease in the uptake values at higher pH values, due to the precipitation of the metal hydroxides in the basic solution<sup>31</sup>.



**Table 1.** Effect of pH on the uptake of the metal ions ( $\text{Cu}^{2+}$ ,  $\text{Cd}^{2+}$ ,  $\text{Co}^{2+}$ ,  $\text{Zn}^{2+}$ ,  $\text{Hg}^{2+}$ ,  $\text{Pb}^{2+}$ ) by the chelating resins **Rciaa91** and **Rciaa73** after 60 minutes.

pH	Capacity (mmol/g resin)											
	Rciaa91						Rciaa73					
	$\text{Cu}^{2+}$	$\text{Cd}^{2+}$	$\text{Hg}^{2+}$	$\text{Co}^{2+}$	$\text{Pb}^{2+}$	$\text{Zn}^{2+}$	$\text{Cu}^{2+}$	$\text{Cd}^{2+}$	$\text{Hg}^{2+}$	$\text{Co}^{2+}$	$\text{Pb}^{2+}$	$\text{Zn}^{2+}$
4	1.36	0.13	2.32	0.42	1.10	0.72	1.08	0.13	2.17	0.15	0.70	0.54
5	1.44	0.27	<b>2.92</b>	0.42	1.13	1.02	1.28	0.20	<b>2.60</b>	0.57	0.97	0.87
6	--	--	2.77	--	1.28	--	--	--	2.50	--	1.12	--
7	1.84	0.65	2.4	<b>1.17</b>	<b>1.53</b>	1.48	1.40	0.53	1.75	<b>0.93</b>	<b>1.28</b>	1.22
8	<b>1.84</b>	0.90	--	1.10	--	<b>1.79</b>	<b>1.40</b>	0.76	--	0.79	--	<b>1.38</b>
9	--	<b>1.00</b>	--	--	--	1.66	--	<b>0.88</b>	--	--	--	1.32
10	1.43	0.53	--	--	--	--	1.28	0.50	--	--	--	--

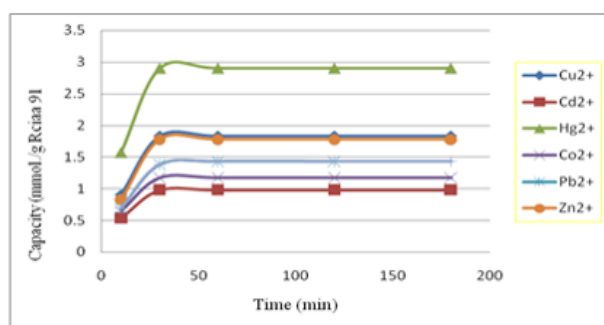
The optimum pH values obtained for the metal ions under study;  $\text{Cu}^{2+}$ ,  $\text{Cd}^{2+}$ ,  $\text{Co}^{2+}$ ,  $\text{Zn}^{2+}$ ,  $\text{Hg}^{2+}$ ,  $\text{Pb}^{2+}$  are 8, 9, 7, 8, 5, 7, respectively.

Table 1 showed that the chelating resins **Rciaa91** and **Rciaa73** absorbed the metal ions in the following order  $\text{Hg}^{2+} > \text{Cu}^{2+} > \text{Zn}^{2+} > \text{Pb}^{2+} > \text{Co}^{2+} > \text{Cd}^{2+}$  each metal at its optimum pH and at the same reaction time and ion concentration. A special feature seen in this study is that  $\text{Hg}^{2+}$  ion showed the highest uptake affinity at low pH compared to the rest of the metal ions under study. This allows separation of  $\text{Hg}^{2+}$  ions, selectively, in the presence of other metal ions.

### 3.3.2 Effect of contact time

The interaction between the resin and metal ion continues until most of effective sites of the resin are occupied by the metal ion. At this point the resin is said to have reached the equilibrium state with the metal ions<sup>32</sup>. The time required to reach the equilibrium state for the uptake processes of each metal ion with the chelating resins **Rciaa91** and **Rciaa73** was evaluated at their optimum pH values. Table 2 and Figures 3 and 4 show the relationship between the uptake processes of each metal ion and the equilibrium reaction time, for the chelating resins **Rciaa91** and **Rciaa73**, respectively. In the case of the chelating resins **Rciaa91**, the equilibrium state was attained within 30 min for all the metal ions and the time required for 50% uptake was about 10 min. On the other

hand, for the chelating resin **Rciaa73**, the equilibrium state was attained within 60 min for the metal ions under investigation and the time required for 50% uptake was about 30 min.



**Figure 3.** Effect of the reaction time on the uptake of the metal ion ( $\text{Cu}^{2+}$ ,  $\text{Cd}^{2+}$ ,  $\text{Hg}^{2+}$ ,  $\text{Co}^{2+}$ ,  $\text{Pb}^{2+}$  and  $\text{Zn}^{2+}$ ) for the resin **Rciaa91**. Resin; 0.05 g, metal ion; 0.005 mol L<sup>-1</sup> and solution volume 50 mL.

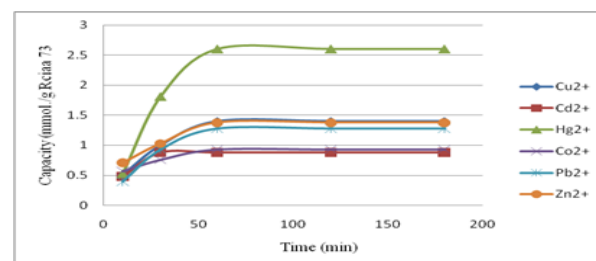


**Figure 4.** Effect of the reaction time on the uptake of the metal ions ( $\text{Cu}^{2+}$ ,  $\text{Cd}^{2+}$ ,  $\text{Hg}^{2+}$ ,  $\text{Co}^{2+}$ ,  $\text{Pb}^{2+}$  and  $\text{Zn}^{2+}$ ) for the resin **Rciaa73**. Resin; 0.05 g, metal ion; 0.005 mol L<sup>-1</sup> and solution volume 50 mL.

**Table 2.** Effect of reaction time on the uptake of the metal ions ( $\text{Cu}^{2+}$ ,  $\text{Cd}^{2+}$ ,  $\text{Co}^{2+}$ ,  $\text{Zn}^{2+}$ ,  $\text{Hg}^{2+}$ ,  $\text{Pb}^{2+}$ ) by the chelating resins **Rciaa91** and **Rciaa73** at optimum pH.

Time (min)	Capacity (mmol/g resin)											
	Rciaa91						Rciaa73					
	$\text{Cu}^{2+}$	$\text{Cd}^{2+}$	$\text{Hg}^{2+}$	$\text{Co}^{2+}$	$\text{Pb}^{2+}$	$\text{Zn}^{2+}$	$\text{Cu}^{2+}$	$\text{Cd}^{2+}$	$\text{Hg}^{2+}$	$\text{Co}^{2+}$	$\text{Pb}^{2+}$	$\text{Zn}^{2+}$
10	0.9	0.54	1.57	0.65	0.69	0.83	0.51	0.48	0.53	0.57	0.39	0.71
30	1.83	0.98	2.90	1.17	1.38	1.78	1.00	0.88	1.81	0.76	0.93	1.03
60	1.83	0.98	2.90	1.17	1.43	1.78	1.40	0.88	2.60	0.93	1.28	1.38
120	1.83	0.98	2.90	1.17	1.43	1.78	1.40	0.88	2.60	0.93	1.28	1.38
180	1.83	0.98	2.90	1.17	1.43	1.78	1.40	0.88	2.60	0.93	1.28	1.38

From the data obtained it could be concluded that the uptake values depend on both the metal ion and the pH values. The uptake capacity of the chelating resins, **Rciaa91** and **Rciaa73** for different metal ions showed a maximum value of  $2.9 \text{ mmol g}^{-1}$  resin and  $2.6 \text{ mmol g}^{-1}$  resin for  $\text{Hg}^{2+}$  ions and a minimum value of  $0.98 \text{ mmol g}^{-1}$  resin and  $0.88 \text{ mmol g}^{-1}$  resin for  $\text{Cd}^{2+}$  ions, respectively. The uptake capacities of the rest of the metal ions were in between for both the chelating resins **Rciaa91** and **Rciaa73** as seen in Figures 3 and 4, respectively.

The differences in the uptake capacities may be attributed to i) the differences in the stability constants of the formed complexes between the different metal ions and the resin<sup>33, 34</sup>. For this reason, the differences in the stability constants may explain the high uptake capacities of  $\text{Hg}^{2+}$  for both the chelating resins, in spite of the large ionic radii of the mercury (II) ion compared to the other ions under investigation, ii) the differences in ionic

radii of the metal ions; the smaller the ion size the easier it can penetrate through the network of the resin<sup>33</sup>. This explains why, the smallest ion  $\text{Cu}^{2+}$ , (ionic radii  $0.72 \text{ \AA}$ ) showed high uptake capacities,  $1.84 \text{ mmol g}^{-1}$  and  $1.40 \text{ mmol g}^{-1}$ , whereas the largest ion  $\text{Cd}^{2+}$ , (ionic radii  $0.97 \text{ \AA}$ ) showed low uptake capacities,  $0.90 \text{ mmol g}^{-1}$  and  $0.88 \text{ mmol g}^{-1}$ , for **Rciaa91** and **Rciaa73**, respectively.

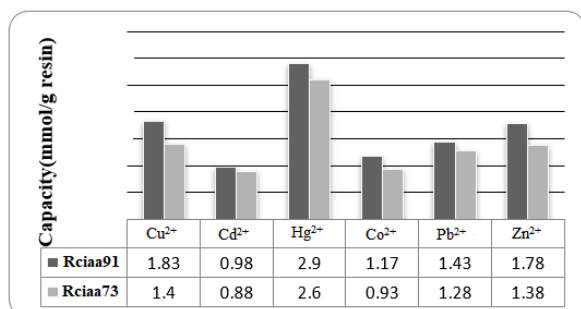
3.4 The effect of compositional ratio of the chelating groups and degree of cross-linking between **Rciaa91** and **Rciaa73** on the uptake processes.

Table 3 and the Figure 5 show the effect of chelating group and degree of cross-linking ratio of **Rciaa91** and **Rciaa73** on the uptake process of the metal ions at the same pH medium, initial metal concentration and reaction time.

**Table 3.** Effect of degree of cross-linking on the uptake of metal ions ( $\text{Cu}^{2+}$ ,  $\text{Cd}^{2+}$ ,  $\text{Hg}^{2+}$ ,  $\text{Co}^{2+}$ ,  $\text{Pb}^{2+}$  and  $\text{Zn}^{2+}$ ) for the resins **Rciaa91** and **Rciaa73** at 60 min.

Chelating resin	Degree of cross-linking (%) by weight	Capacity (mmol/g resin)					
		$\text{Cu}^{2+}$	$\text{Cd}^{2+}$	$\text{Hg}^{2+}$	$\text{Co}^{2+}$	$\text{Pb}^{2+}$	$\text{Zn}^{2+}$

<b>Rciaa91</b>	10	1.84	0.98	2.9	1.17	1.43	1.78
<b>Rciaa73</b>	30	1.4	0.88	2.6	0.93	1.28	1.38
uptake difference (%)		24	10	10	21	10	22



**Figure 5.** A comparative result on the uptake of metal ions (Cu<sup>2+</sup>, Cd<sup>2+</sup>, Hg<sup>2+</sup>, Co<sup>2+</sup>, Pb<sup>2+</sup> and Zn<sup>2+</sup>) by the resins **Rciaa91** and **Rciaa73**.

The results obtained indicated that the resin **Rciaa91** has higher uptake efficiency than **Rciaa73** at the same conditions. This is due to the difference in the compositional ratio of chelating groups and degree of cross-linking of the chelating resins **Rciaa91** and **Rciaa73**. The resin **Rciaa91** with ratio (9:1) by weight, has about 20% of coordinating groups RCH=N-C<sub>6</sub>H<sub>4</sub>-COOH more than the resin **Rciaa73** with compositional ratio (7:3) by weight. Therefore, the low metal ion uptake capacity of the chelating resin **Rciaa73** could be attributed to its higher degree of cross linking. This presumably hinders the approach of the metal ions to the polymeric matrix and, hence, limits the chelating reaction<sup>35</sup>.

The uptake of the resin **Rciaa91** was about 20% more than that of the resin **Rciaa73** for the small metal ions under investigation (Cu<sup>2+</sup>, Co<sup>2+</sup>, Zn<sup>2+</sup>) whose ionic radii was nearly 0.7 Å. This ratio is nearly close to the theoretical ratio of chelating groups between the two resins. On the other hand, the uptake of the large ions (Cd<sup>2+</sup>, Hg<sup>2+</sup> and Pb<sup>2+</sup>) with ionic radii of about 1 Å, by the resin **Rciaa91** was about 11% more than that of the resin **Rciaa73**. This shortage in uptake capacity maybe due to the larger ionic volume of metal ions (Cd<sup>2+</sup>, Hg<sup>2+</sup> and Pb<sup>2+</sup>) and the increasing of degree of cross linking in the resin **Rciaa73**<sup>26, 33</sup>.

### 3.5 The effect of the degree of cross linking on the optimum reaction time for the uptake processes.

The data in the Table 2 and Figures 3 and 4 showed that the resin **Rciaa91** with a lower degree of cross linking reached the optimum reaction time for the uptake process at half time period compared to the resin **Rciaa73**. For example, the equilibrium state for the uptake of Cu<sup>2+</sup> ions by **Rciaa91** at the optimum pH 8 was attained after 30 min, whereas the equilibrium state for the uptake of Cu<sup>2+</sup> ions by **Rciaa73** was reached after 60 min. Also, it was calculated from the data obtained that the time required to achieve 50% of the metal ion uptake was within 5 min for **Rciaa91**, whereas, it was within 20 min for **Rciaa73**.

The comparison between the optimum reaction time for the resins, **Rciaa91** and **Rciaa73**, which have the same chemical structure, but different degree of cross-linking proved that, the higher the degree of cross-linking the higher the optimum reaction time, at the same pH medium.

The resin **Rciaa73** has about 200% more cross linking through RCH=NC<sub>6</sub>H<sub>4</sub>N=CHR than the resin **Rciaa91**. A high degree of cross-linking makes the polymer chains more rigid and more hindering for the metal ions to penetrate the network of the resin in order to act with the active sites. This in turn, will lead to a decrease in the rate of uptake process and increase in the time required to reach the equilibrium state during the uptake<sup>26, 33</sup>.

### 3.6 Thermal Studies

The TGA and DTA curves of the prepared **Rciaa91** and **Rca73** resins are given in Figures 6.1 and 6.2. These curves characterize and compare the thermal degradation of these two resins at 10 °C min<sup>-1</sup> heating rate, under nitrogen and over the range 20-800 °C. For the evaluation of the thermal degradation kinetics parameters at a single heating rate (10 °C min<sup>-1</sup>), the activation energy ( $E_a$ ) and pre-exponential factor ( $Z$ ) are determined by using the Coats-Redfern method<sup>36</sup> for the reaction order  $n \neq 1$ . When the Coats-Redfern method is linearized for a correctly-chosen order of reaction ( $n$ ) yields the activation energy ( $E_a$ ) from the slope of the equation:



$$\log \left[ \frac{1 - (1 - \alpha)^{1-n}}{T^2(1-n)} \right] = \log \left[ \frac{ZR}{qE_a} \left( 1 - \frac{2RT}{E_a} \right) \right] - \frac{E_a}{2.303RT} \text{ for } n \neq 1 \rightarrow 1$$

where:  $\alpha$  = fraction of weight loss,  $T$  = temperature (K),  $Z$  = pre-exponential factor,  $R$  = molar gas constant,  $q$  = heating rate and  $n$  = reaction order; estimated by Horovitz-Metzger method<sup>37</sup>.

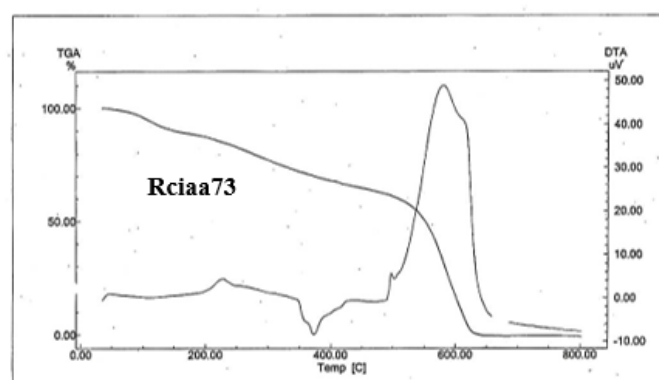
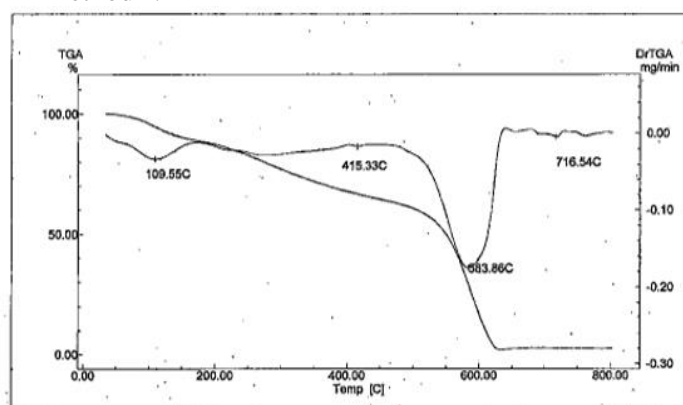
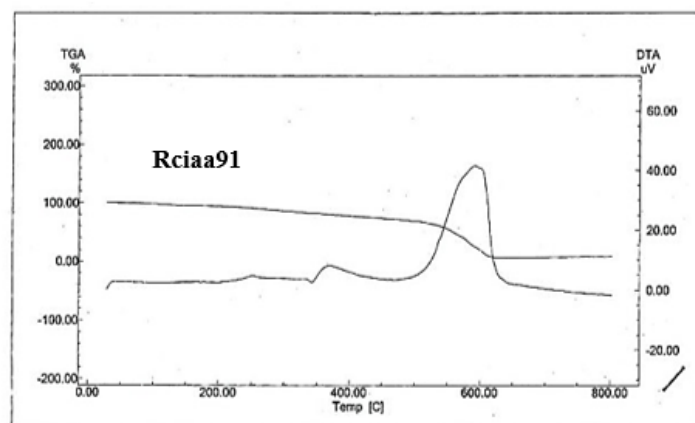


Figure 6.2: DTA thermograms of **Rciaa91** and **Rciaa73** in nitrogen at  $10\text{ }^{\circ}\text{C min}^{-1}$  heating rate.

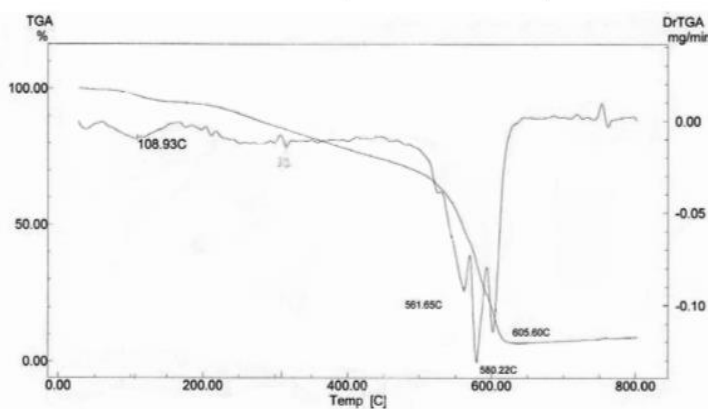


Figure 6.1. TGA thermograms of **Rciaa91** and **Rciaa73** in nitrogen at  $10\text{ }^{\circ}\text{C min}^{-1}$  heating rate.

The thermodynamic parameters of the thermal degradation step; enthalpy ( $\Delta H^*$ ), entropy ( $\Delta S^*$ ), and Gibbs energy ( $\Delta G^*$ ) of activation are calculated using the following standard equations:

$$\Delta S^* = R \ln \frac{Zh}{kT_{\max}}$$

$$\Delta H^* = E_a - RT_{\max}$$

$$\Delta G^* = \Delta H^* - T_{\max} \Delta S^*$$

The characteristics of the thermal degradation of these two resins recorded on the TG/DTG/DTA curves, their kinetics and thermodynamics parameters extracted from these curves are given in Tables 4 and 5.

The thermal degradation TG curves of **Rciaa91** and **Rciaa73** resin (Figures 6.1 and 6.2) showed a very slow and continuous mass bleeding (i.e. no plateau from the start up to about 450 °C) of about 37.7% and 27.8%, respectively. Consequently, very small and weak DTG peaks are observed on the DTG curves of these resins and this is indicative to the very slow degradation process in both resins

at the about 35-450 °C range. Therefore, the prominent steps of these two resins that occur at about 470-641 °C range with large and strong DTG peak at 580 °C (**Rciaa91**) and 584 °C (**Rciaa73**) are considered as characteristic steps for which the thermal degradation, kinetics and thermodynamics parameters are determined and hence compared (Tables 4 and 5).

The **Rciaa91** resin showed a mass loss (61.3%) at the prominent step (470-634 °C) with strong  $T_{DTG}$  at 584 °C and exothermic  $T_{DTA}$  peak at 580 °C. The calculated activation energy  $E_a$  of the **Rciaa91** resin for this prominent step is 184 kJ mol<sup>-1</sup>, while -167 J K<sup>-1</sup> mol<sup>-1</sup>, 83 kJ mol<sup>-1</sup> and 226 kJ mol<sup>-1</sup> are the values of entropy ( $\Delta S^*$ ), enthalpy ( $\Delta H^*$ ), and Gibbs energy ( $\Delta G^*$ ) changes. The prominent step (480-641 °C) of the **Rciaa73** resin showed also exothermic mass loss (64.7%) with strong  $T_{DTG}$  (580 °C) and  $T_{DTA}$  (592 °C). The activation energy  $E_a$ , entropy ( $\Delta S^*$ ), enthalpy ( $\Delta H^*$ ), and Gibbs energy ( $\Delta G^*$ ) changes are 180 kJ mol<sup>-1</sup>, -211 J K<sup>-1</sup> mol<sup>-1</sup>, 49 kJ mol<sup>-1</sup> and 226 kJ mol<sup>-1</sup>, respectively.

**Table 4.** Characteristic parameters of the thermal degradation of the resins **Rciaa91** and **Rciaa73**.

Resin	TGA				DTA		$E_a$ kJ mol <sup>-1</sup>
	$\Delta m$ %	$T_i$ °C	$T_f$ °C	$T_{DTG}$ °C	$T_{DTA}$ °C	Peak	
<b>Rciaa91</b>	61.3	470	634	584	580	exo	184
<b>Rciaa73</b>	64.7	480	641	580	592	exo	180

**Table 5.** Kinetic and thermodynamic parameters of the thermal degradation of the resins **Rciaa91** and **Rciaa73**

Resin	$r$	$n$	$T_{\max}$ °C	$Z$ s <sup>-1</sup>	$E_a$ kJ mol <sup>-1</sup>	$\Delta S^*$ kJ mol <sup>-1</sup>	$\Delta H^*$ kJ mol <sup>-1</sup>	$\Delta G^*$ kJ mol <sup>-1</sup>
<b>Rciaa91</b>	0.997	0.9	584	$2.9 \times 10^{17}$	184	80.6	176.9	108.3
<b>Rciaa73</b>	0.998	0.7	580	$8.3 \times 10^{16}$	180	70.3	172.9	112.9

If the initial molecular structure destruction temperature ( $T_i$ ) of the **Ricaa91** and **Ricaa73** resin is taken as a measure of the thermal stability, these two resins are of similar thermal stability for their similar  $T_i$  (35 °C). It can be concluded that although the two resins **Ricaa91** and **Ricaa73** are of similar chemical structure but different degree of cross-linking, their TGA curves and the data extracted from them (Tables 4 and 5) indicate almost similar thermal degradation behavior, kinetics and thermodynamics parameters as well as similar thermal stability regardless the difference in the degree of the cross-linking 1:3 (**Rciaa91**:**Rciaa73**). The resin **Rciaa91** losses 37.7% of its mass slowly and 61.3% rapidly with 1% residue, while **Rciaa73**

losses 28% slowly and 64.7% rapidly with 7.5% residue. This difference in mass loss degradation process may be due to the cross-linking variation.

#### 4. Conclusions

The effect of the compositional ratio of the chelating groups and the degree of the cross-linking of the Schiff base chelating resins, **Rciaa91** and **Rciaa73** on the uptake behavior of the heavy metal ions (Cu<sup>2+</sup>, Cd<sup>2+</sup>, Hg<sup>2+</sup>, Co<sup>2+</sup>, Pb<sup>2+</sup> and Zn<sup>2+</sup>) was the main aim of this research. A special feature observed in this study was that Hg<sup>2+</sup> ions showed the highest uptake affinity at low pH compared to the rest of the metal ions under study for both

resins, **Rc1aa91** and **Rc1aa73**. The difference in the uptake affinity of the chelating resins may be due to i) the ionic radii of the metal ions; the smaller the ion size the easier it can penetrate through the network of the resin, ii) the stability constants which explains the high uptake capacities of  $\text{Hg}^{2+}$  for both the chelating resins, in spite of the large ionic radii of the mercury (II) ion compared to the other ions under investigation.

When comparing between the uptake affinity and the optimum reaction time for the chelating resins **Rc1aa91** and **Rc1aa73**, which have the same chemical structure, but different degree of cross linking, one concludes that the higher the degree of cross-linking the higher the optimum reaction time and the lower the uptake affinity towards the heavy metal ions.

The chelating resins showed good thermal stability. The thermal degradation behavior and the kinetic parameters of the resin **Rc1aa91** and **Rc1aa73** are almost similar, indicating that the differences in the degree of cross-linking are almost of no significant effects.

## 5. References

- [1] Shah, B. A., Shah, A. V., Shah, P. M., Analytical and Morphology Studies of Phthalic acid-Formaldehyde Resorcinol as Chelating Resin, *Malaysian Polymer Journal (MPJ)* 4 (2) (2009) 1-12.
- [2] Cavaco, S. A., Fernandes, S., Augusto, C. M., Quina, M. J., Gando-Ferreira, L. M., Evaluation of chelating ion-exchange resins for separating Cr(III) from industrial effluents, *J. Hazard. Mater.* 169 (2009) 516-523. <https://doi.org/10.1016/j.jhazmat.2009.03.129>.
- [3] Dikshit, D., Polymorphisms in DNA Sequence and Personalized Alternative Herbal Drugs, *Orient Journal of Chemistry (OJC)* 29 (1) (2013) 305-307.
- [4] Hassan, R., Arida, H., Montasser, M., Abdel Latif N., Synthesis of New Schiff Base from Natural Products for Remediation of Water Pollution with Heavy Metals in Industrial Areas, *J. Chem.* 2013 (2013) 1-10. <https://doi.org/10.1155/2013/240568>.
- [5] Cheng-Chien W., Chun-Chih W., Synthesis and characterization of chelating resins with amino moieties and application on removal of copper(II) from EDTA complexes, *J. Appl. Polym. Sci.* 97 (2005) 2457-2468. <https://doi.org/10.1002/app.22019>.
- [6] Shareef, B. A., Waheed, I. F., Jalaot, K. K., Preparation and Analytical Properties of 4-Hydroxybenzaldehyde, Biuret and Formaldehyde Terpolymer Resin, *Orient Journal of Chemistry (OJC)* 29 (4) (2013) 1391-1397. <https://doi.org/10.13005/ojc/290414>.
- [7] Al-Yusufy, F. A., Othman, M. K., Al-Qadri, F. A., Synthesis and Metal Ion Uptake Studies of Formaldehyde and Furfuraldehyde-Condensed Phenol-Schiff Base Chelating Resins, *Sana'a Univ. J. Sci. & Technol.*, 2 (1) (2005) A(9-19).
- [8] Monier, M., Abdel-Latif, D. A., El-Reash, Y. A., Ion-imprinted modified chitosan resin for selective removal of Pd(II) ions, *J. Colloid Interface Sci.* 469 (2016) 344-354. <https://doi.org/10.1016/j.jcis.2016.01.074>.
- [9] Urbano, B. F., Rivas, B. L., Sorption properties of chelating polymer-clay nano-composite resin based on iminodiacetic acid and montmorillonite: water absorbency, metal ion uptake, selectivity, and kinetics, *J. Chem. Technol. Biotechnol.* 89 (2) (2014) 249-258. <https://doi.org/10.1002/jctb.4109>.
- [10] Veliscek-Carolan, J., Separation of actinides from spent nuclear fuel: A review, *J. Hazard. Mater.* 318 (2016) 266-281. <https://doi.org/10.1016/j.jhazmat.2016.07.027>.
- [11] Ling, C., Liu, F. Q., Xu, C., Chen, T. P., Li, A. M., An Integrative Technique Based on Synergistic Coremoval and Sequential Recovery of Copper and Tetracycline with Dual-Functional Chelating resin: Roles of Amine and Carboxyl Groups, *ACS Appl. Mater. Interfaces* 5 (22) (2013) 11808-11817. <https://doi.org/10.1021/am403491b>.
- [12] Laaksonen, T., Heikkinen, S., Wähälä, K., Synthesis of Tertiary and Quaternary Amine Derivatives from Wood Resin as Chiral NMR Solvating Agents, *Molecules* 20 (2015) 20873-20886. <https://doi.org/10.3390/molecules201119732>.
- [13] Monier, M., Adsorption of  $\text{Hg}^{2+}$ ,  $\text{Cu}^{2+}$  and  $\text{Zn}^{2+}$  ions from aqueous solution using formaldehyde cross-linked modified chitosan-

thioglyceraldehyde Schiff's base, *Int. J. Biol. Macromol.* 50 (3) (2012) 773-781. <https://doi.org/10.1016/j.ijbiomac.2011.11.026>.

[14] Donia, A. M., Atia, A. A., Elwakeel, K. Z., Selective separation of mercury(II) using magnetic chitosan resin modified with Schiff's base derived from thiourea and glutaraldehyde, *J. Hazard. Mater.* 151 (2-3) (2008) 372-379. <https://doi.org/10.1016/j.jhazmat.2007.05.083>.

[15] Yang, W., Zheng, F., Xue, X., Lu, Y., Investigation into adsorption mechanisms of sulfonamides onto porous adsorbents, *J. Colloid Interface Sci.* 362 (2) (2011) 503-509. <https://doi.org/10.1016/j.jcis.2011.06.071>.

[16] El-Reash, Y.A., Otto, M., Kenawy, I.M., Ouf, A.M., Adsorption of Cr(VI) and As(V) ions by modified magnetic chitosan chelating resin, *Int. J. Biol. Macromol.* 49 (4) (2011) 513-522. <https://doi.org/10.1016/j.ijbiomac.2011.06.001>.

[17] Othman, M. K., Al-Qadri, F. A., Al-Yusufy, F. A., Synthesis, physical studies and uptake behavior of: Copper(II) and lead(II) by Schiff base chelating resins, *Spectrochim. Acta A Mol. Biomol. Spectrosc.* 78 (5) (2011) 1342-1348. <https://doi.org/10.1016/j.saa.2010.12.073>.

[18] Oo, C. W., Osman, H., Fatinathan, S., Md. Zin, M. A., The Uptake of Copper(II) Ions by Chelating Schiff Base Derived from 4-Aminoantipyrine and 2-Methoxybenzaldehyde, *International Journal of Nonferrous Metallurgy (IJNM)* 2 (2013) 1-9. <https://doi.org/10.4236/ijnm.2013.21001>.

[19] M. Singanan, Biosorption of Hg(II) ions from synthetic wastewater using a novel biocarbon technology, *Eviron. Eng. Res.* 20 (1) (2015) 33-39. <https://doi.org/10.4491/eer.2014.032>.

[20] Hamzaa, M. F., Abdel-Monemb, Y. K., Farag, N. M., El-Tanbouly, A. M., Studies on the Recovery of Cu (II) and U (VI) on Highly Adsorptive Modified Magnetic Amine Resins from Dolostone Leachate Solution, *International Journal of Sciences: Basic and Applied Research (IJSBAR)*, 30 (1) (2016) 149-166.

[21] Daşbaşı, T., Saçmac, Ş., Şahan, S., Kartal, Ş., Ülgen, A., Synthesis, characterization and application of a new chelating resin for on-line

separation, preconcentration and determination of Ag(I) by flame atomic absorption spectrometry, *Talanta* 103 (2013) 1-7. <https://doi.org/10.1016/j.talanta.2012.09.017>.

[22] Haron, M. J., Yunus, W. M. Z., Removal of fluoride ion from aqueous solution by a cerium-poly (hydroxamic acid) resin complex, *J. Environ. Sci. Health. A.* 36 (2001) 727-734. <https://doi.org/10.1081/ESE-100103756>.

[23] El-Hamshary, H., El-Newehy, M. H., Al-Deyab, S. S., Oxidation of phenol by hydrogen peroxide catalyzed by metal-containing poly (amidoxime) grafted starch, *Molecules* 16 (2011) 9900-9911. <https://doi.org/10.3390/molecules16129900>.

[24] Dragan, E.S., Apopei Loghin, D. F., Cocarta, A. I., Efficient Sorption of Cu<sup>2+</sup> by Composite Chelating Sorbents Based on Potato Starch-graft-Polyamidoxime Embedded in Chitosan Beads, *ACS Appl. Mater. Interfaces* 6 (19) (2014) 16577-16592. <https://doi.org/10.1021/am504480q>.

[25] Hazer, O., Kartal, S., Synthesis of a novel chelating resin for the separation and preconcentration of uranium (VI) and its spectrophotometric determination, *Anal. Sci.* 25 (2009) 547-551. <https://doi.org/10.2116/analsci.25.547>.

[26] Othman, M. K., Ph. D. Thesis, Preparation and Thermal Behavior Studies of Some New Polymers and Their Uses in Metal Complexes and Heavy Metal ions Removal from Aqueous Solutions, Zagazig University, Benha Branch, Faculty of Science, Chemistry Department, 2003.

[27] West, T. S., *Complexometry with EDTA and Related Reagents*, BDH Chemicals Ltd, 3rd ed., 1969.

[28] Peters, D. G., Hayes, J. M., Hieftje, G. M., *Chemical Separations and Measurements Theory and Practice of Analytical Chemistry*, Saunders Company, 3rd ed., 1974.

[29] El-Sayed, G. O., Dessouki, H. A., Ibrahiem, S. S., Removal of Zn(II), Cd(II) and Mn(II) from aqueous solutions by adsorption on maize stalks, *Malaysian Journal of Analytical Sciences (MJAS)* 15(1) (2011) 8-21.

[30] Silverstein, R. M., Bassler, G. C., Morrill, T. C., Spectroscopic Identification of Organic Compounds, John Wiley, New York, (1981).

[31] Bhatt, R. R., Shah, B. A., Shah, A. V., Uptake of heavy metal ions by chelating ion-exchange resin derived from p-hydroxybenzoic acid-formaldehydesorcinol: synthesis, characterization and sorption dynamics, The Malaysian Journal of Analytical Sciences (MJAS) 16 (2) (2012) 117-133.

[32] Naiya, T. K., Bhattacharya, A. K., Das, S. K., Adsorptive removal of Cd(II) ions from aqueous solutions by rice husk ash, Environ. Prog. Sustain. Energy 28 (4) (2009) 535–546. <https://doi.org/10.1002/ep.10346>.

[33] Cotton, F. A., Wilkinson, G., Advanced Inorganic Chemistry; A Comprehensive Text, John Wiley & Sons, New York, 3rd ed., 1972.

[34] Malakul, P., Srinivasan, K., Wang, Y. H., Metal Adsorption and Desorption Characteristics of Surfactant-Modified Clay Complexes, Ind. Eng. Chem. Res. 37(11) (1998) 4296-4301. <https://doi.org/10.1021/ie980057i>.

[35] Lezzi, A., Cobianco, S., Roggero, A., Synthesis of thiol chelating resins and their adsorption properties toward heavy metals ions, J. Polym. Sci., Part A 32 (10) (1994) 1877-1883. <https://doi.org/10.1002/pola.1994.080321008>.

[36] Coats, A. W., Redfern, J. P., Kinetic Parameters from Thermogravimetric Data, Nature 201 (1964) 68-69.

[37] Horowitz, H. H., Metzger, G., A New Analysis of Thermogravimetric Traces, Anal. Chem. 35 (10) (1963) 1464-1468. <https://doi.org/10.1021/ac60203a013>.